Sharpness of the Berezinskii-Kosterlitz-Thouless Transition in Disordered NbN Films

Alexander Weitzel,[1,*] Lea Pfaffinger,[1,*] Ilaria Maccari,[2] Klaus Kronfeldner,[1] Thomas Huber,[1] Lorenz Fuchs,[1] James Mallord,[1] Sven Linzen,[3] Evgeni Il'ichev,[3] Nicola Paradiso,[1] and Christoph Strunk[1,†]

[1]*Institute for Experimental and Applied Physics, University of Regensburg, D-93040 Regensburg, Germany*

[2]*Department of Physics, Stockholm University, SE-10691 Stockholm, Sweden*

[3]*Leibniz Institute of Photonic Technology, D-07745 Jena, Germany*

(Received 12 March 2023; accepted 21 September 2023; published 1 November 2023)

We present a comprehensive investigation of the Berezinskii-Kosterlitz-Thouless transition in ultrathin strongly disordered NbN films. Measurements of resistance, current-voltage characteristics, and kinetic inductance on the very same device reveal a consistent picture of a sharp unbinding transition of vortex-antivortex pairs that fit standard renormalization group theory without extra assumptions in terms of inhomogeneity. Our experiments demonstrate that the previously observed broadening of the transition is not an intrinsic feature of strongly disordered superconductors and provide a clean starting point for the study of dynamical effects at the Berezinskii-Kosterlitz-Thouless transition.

DOI: 10.1103/PhysRevLett.131.186002

In two dimensions, the superfluid transition is governed by the presence of thermally excited vortex-antivortex pairs [1,2]. For superfluid ^{4}He films, the defining features of the Berezinskii-Kosterlitz-Thouless (BKT) transition are well understood [3,4]. In thin-film superconductors an analogous behavior is expected, the transition being caused by dissociation of vortex-antivortex pairs. The transition is manifested as a discontinuous jump in the superfluid phase stiffness J_s at a temperature T_{BKT} below the mean-field transition temperature T_{c0} [5,6]. Moreover, below T_{BKT} the voltage-current characteristics $V(I)$ are nonlinear, $V \propto I^{\alpha(T)}$, with a temperature dependent exponent α [7]. In the thermodynamic limit, a linear voltage response regime exists above T_{BKT} only.

Physics of the BKT transition is controlled by two energy scales [8]. In order to thermally excite a vortex-antivortex pair in a film, the energy cost for the generation of vortex cores (also called vortex fugacity) $\mu \propto \xi^2$, as well as the energy scale for the pair dissociation $J_s \propto 1/\lambda^2$, must be sufficiently small. Here, ξ and λ are the coherence length and magnetic penetration depth, respectively. In the dirty limit, both ξ^2 and $1/\lambda^2$ are proportional to the elastic mean free path. Owing to their small μ and J_s, ultrathin films of strongly disordered superconductors are the preferred choice for materials that feature a large separation between T_{BKT} and the mean-field critical temperature T_{c0}.

In the past $J_s(T)$ and $V(I)$ were studied for InO and NbN thin films [9–11] using the two-coil method [12] and standard transport measurements. The two-coil method requires circular films with typical 10 mm diameter, while for dc transport long strips are needed. Hence, $J_s(T)$ and $R(T)$ could not be studied in the same devices limiting the validity of consistency checks. While a qualitative agreement with original theory was observed, measurements of strongly disordered NbN films always displayed a broadening of the BKT transition, far stronger than expected for, e.g., finite size effects alone [8,13]. At present, such broadening is believed to be typical for highly disordered superconducting films that are known to feature *emergent granularity* [14–19]. Local variations of the modulus of the order parameter and superfluid stiffness could, in principle, explain the observed smearing of the expected discontinuous jump in J_s. On the other hand, such smearing introduces an additional free parameter that inevitably obscures the quantitative analysis.

Within the generally accepted picture, individual signatures of the BKT transition have been observed [9–13,20–29]. In recent years, however, it turned out that each of these signatures is affected by experimental subtleties that need to be controlled in order to reliably test the level of consistency [30,31]. The most popular signature, the nonlinearity of $V(I)$, is also the most difficult to interpret, as many other effects affect it. For example, any fluctuation induced broadening of the resistive transition leads to nonlinear $V(I)$ via heating. This can mimic a power-law behavior, in particular close to the normal state resistance and for materials with $T_{c0} \lesssim 1$ K [32]. To address this issue, a set of techniques is desirable that do not extrinsically broaden the transition and allows for all types of measurements to be performed on the very same device.

In this Letter, we observe a sharp BKT transition in strongly disordered NbN films while the resistive transition is smeared over several kelvins. Using a low-frequency resonator technique compatible with four terminal dc measurements, we unambiguously identify the BKT and mean-field transition temperatures. We find an excellent agreement of both T_{BKT} and T_{c0} extracted from dc resistance and superfluid stiffness in disjunct temperature regimes. The inductively measured stiffness shows excellent

agreement with the values extracted from nonlinear dc transport, provided that voltages are sufficiently small. Our results provide a solid basis for the study of more complex nonequilibrium properties of ultrathin and strongly disordered superconductors.

Our NbN films are grown by atomic layer deposition (ALD, 75 cycles) [33] with a thickness $d = 3.5 \pm 0.3$ nm on top of a thermally oxidized silicon wafer. Over several months at ambient conditions, the NbN film gradually oxidizes, signaled by an increase of the sheet resistance. Using standard electron beam lithography and selective etching techniques we prepared long (∼100–200 squares) meander structures of width ranging from 10–200 μm with a total kinetic inductance of ∼100 nH. The samples are mounted into a cold tank circuit, whose resonance frequency provides access to the sheet kinetic inductance $L_\square$ of the sample [34,35]. The resonance frequency of the circuit varies between 0.5–3 MHz, depending on $L_\square$. From the kinetic inductance, the superfluid stiffness is inferred as

$$J_s = \frac{\hbar^2 d}{4e^2 k_B \mu_0 \lambda^2} = \frac{\hbar^2}{4e^2 k_B L_\square}, \tag{1}$$

where h is the Planck's constant, e the elementary charge, k_B the Boltzmann's constant, field, and μ_0 being the vacuum permeability. The parameters of our films are well in line with those of [13,38], albeit with lower thickness for the same values of $k_F\ell$ and T_{c0}. Additional voltage probes allow for measurement of dc $V(I)$ characteristics on the same device. Resistance values were always extracted from the linear regime of $V(I)$.

We start by establishing dc transport properties. Figure 1 shows resistance as function of temperature for a typical meander. The transition is strongly broadened by fluctuations of both amplitude and phase fluctuations of the order parameter [35,39–43].

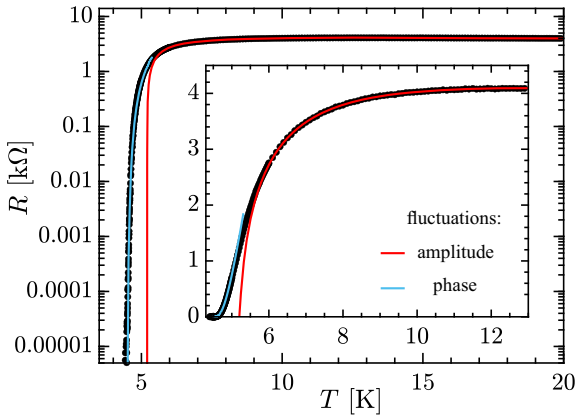

FIG. 1. Sheet resistance, $R(T)$, as function of temperature of a 3.5 nm thick, 10 μm wide, and 2 mm long NbN meander on a logarithmic scale. In the normal state, we measure $R_N = 4.093$ kΩ at 15 K and an electron density $n \simeq 4.5 \times 10^{22}$ cm^{-3} and $k_F\ell \simeq 2$ [35]. Red line, fit including amplitude fluctuations above mean-field critical temperature $T_{c0} = 5.203$ K; blue line, fit to square-root-cusp expression corresponding to $T_{\mathrm{BKT}} = 4.471$ K and $b = 0.76$ (see text). Inset: linear scale of R axis emphasizes amplitude fluctuations.

Fitting $R(T)$ in Fig. 1 for $R > 0.6R_N$ (red line) reveals a mean-field transition temperature $T_{c0} = 5.203$ K (see Ref. [35] for details). Below T_{c0}, phase fluctuations of the order parameter generate resistance, where $R(T)$ has the square-root-cusp form $R(T) \propto \exp(b/\sqrt{T/T_{\mathrm{BKT}} - 1})$ [5,7,35,39–42]. Good agreement is found between theory (blue line) and experiment. Very similar results are found also for other devices with different width and length [35]. According to Halperin-Nelson theory, $V(I,T)$ takes the form [7]

$$V(I,T) = A(T)\, I^{\alpha(T)}, \tag{2}$$

with exponent $\alpha(T) = \pi J_s(T)/T + 1$ and prefactor $A(T)$. Hence, power-law behavior of $V(I)$ characteristics below T_{BKT} is another hallmark of the BKT transition. Increasing temperature decreases J_s and thus α. At the universal transition point $\alpha = 3$ (dashed in Fig. 2) a characteristic jump to $\alpha = 1$ is predicted.

In Fig. 2 we present the evolution of $V(I)$ with temperature. At low temperatures and voltages the double-logarithmic plot reveals the expected power-law dependence. Above T_{BKT} and for sufficiently low current $V(I)$ is expected to be linear. The linear regime is limited first by current-induced dissociation of vortex-antivortex pairs, leading again to power-law behavior of $V(I)$, but now with values of α smaller than 3. Note that the voltage level is orders of magnitude below $R_N I$ (red line in top left corner of Fig. 2).

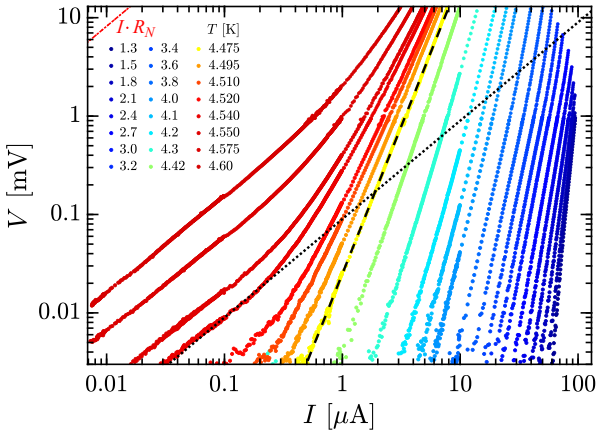

FIG. 2. Voltage-current $[V(I)]$ characteristics at different temperatures. When collecting $V(I)$ over a wide range of current, we used fast sweeps (few s) in order to avoid heating of the chips. Straight lines in log-log display indicate power-law behavior $V \propto I^{\alpha(T)}$, where α is related to $J_s(T)$ [7]. Dotted and dashed black lines correspond to $\alpha = 1$ and 3, respectively. Red solid line in the upper left corner corresponds to $V = R_N I$ in the normal state. Slope $\alpha = 3$ corresponds to $T = 4.475$ K (yellow). $J_s(T)$ extracted from the power-law exponents $\alpha(T)$ is displayed in Fig. 3.

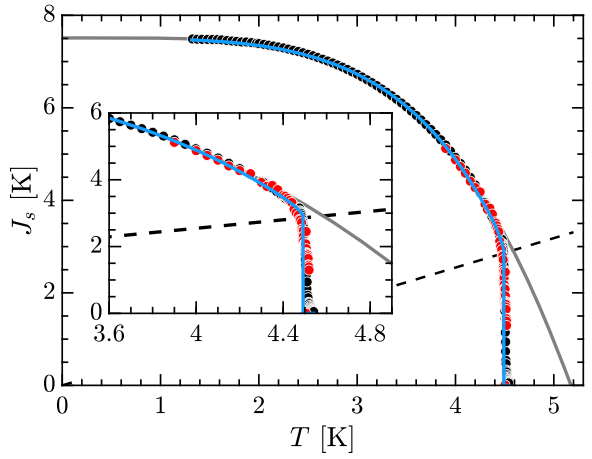

FIG. 3. Superfluid stiffness, J_s, vs temperature, T, for the same device as in Figs. 1 and 2. Black dots, J_s extracted from kinetic inductance; red, J_s extracted from nonlinear IV characteristics (Fig. 2); black, BCS fit of low temperature part, light blue: Renormalization group calculation, dashed black: Nelson-Kosterlitz universal line. Inset: Zoom to the critical region near the jump. The fit parameters for the BCS fit are: $T_{c0} = 5.175$ K, $\Delta(0)/k_B = 13.04$ K and $J_s(0) = 7.511$ K. From $J_s(0)$ we extract $\lambda(0) = 1.71$ μm (Eq. (1). The intersection of the data points with the universal line occurs at $T_{\mathrm{BKT}} = 4.488$ K. The value of the vortex core energy extracted from the RG-fit is $\mu = 19.0$ K.

At higher temperatures and in a wider voltage range $V(I)$ turns out to be much more complex [35,39,40]. At currents exceeding 10 μA and $T \gtrsim T_{\mathrm{BKT}}$ heating effects start to play a role, rendering the $V(I)$-characteristics very complex and even dependent on the speed of current sweeps [35]. Above T_{BKT} the linear part of $V(I)$ may be buried in the background noise, mimicking power-law behavior. Both above and below T_{BKT}, heating effects can affect the observed power law exponent. Based on $V(I)$-characteristics *alone*, it is thus very hard to judge whether values for $J_s(T)$ and even T_{BKT} are correct when extracted from $\alpha(T)$.

As a consistency check, $J_s(T) = T[\alpha(T) - 1]/\pi$ extracted from $V(I)$ is plotted as red dots in Fig. 3 together with $J_s(T)$ (black dots) measured in equilibrium via the kinetic inductance $L_{\square}(T)$. The excellent agreement between the two independent data sets ensures that $\alpha(T)$ was extracted in the right regime of the $V(I)$-characteristics and confirms the validity of our analysis. Very close to the universal transition point at $\pi J_s(T_{\mathrm{BKT}}) = 2T_{\mathrm{BKT}}$ (dashed line), $J_s(T)$ drops to zero within 50 mK. The BKT transition is thus much sharper than in previous experiments on ultrathin NbN films [10,21,38]. Also T_{c0} and T_{BKT} obtained from $R(T)$ ($T > T_{\mathrm{BKT}}$) and $J_s(T)$ ($T < T_{\mathrm{BKT}}$) match within 1% even though data were obtained in disjunct temperature intervals.

The gradual decrease of J_s towards higher T can be described by Bardeen-Cooper-Schrieffer (BCS) theory [10,13]

$$J_s(T) = J_s(0)\,\Delta(T)/\Delta(0) \times \tanh[\Delta(T)/(2k_BT)] \quad (3)$$

(gray line), which accounts for the depletion of J_s by quasiparticle excitations. In order to obtain a good match, it is established practice [10,13] to use $J_s(0)$, $\Delta(0)$, and T_{c0} as independent fitting parameters [35]. The best fit is obtained for $T_{c0} = 5.175$ K, $J_s(0) = \beta J_{\mathrm{BCS}}(0)$, and $\Delta(0) = \gamma 1.764 k_B T_{c0}$ with $\beta = 0.7304$, $\gamma = 1.432$. While T_{c0} agrees within 30 mK or 0.5% with the value obtained from the amplitude fluctuations of the order parameter (Fig. 1), the ratio $\Delta(0)/k_BT_{c0} = 2.521$ exceeds the BCS value of 1.764 as observed earlier [10,21,38,44].

Moreover, $J_s(0)$ is smaller than the dirty limit BCS prediction $J_{\mathrm{BCS}}(0) = \pi\hbar\Delta(0)/(4e^2k_BR_N)$, consistent with the conjectured suppression of $J_s(0)$ by phase fluctuations [38]. The ratio $R_NJ_s(0)/T_{c0} = 5.940 \pm 0.3$ kΩ for several of our films with $R_N \simeq 4$ kΩ agrees within a few percent with the BCS value of $1.764\pi\hbar/(4e^2) = 5.692$ kΩ [35]. This indicates that disorder effects in $J_s(0)/T_{c0}$ are accounted for by R_N alone, while both $J_s(0)$ and T_{c0} substantially differ from their dirty-limit BCS expressions. An independent confirmation of the value of $\Delta(0)$ is highly desirable. Based on direct measurements of $\Delta(0)$ via scanning tunneling spectroscopy (STS), Carbillet *et al.* proposed an interpretation of the large $\Delta(0)/k_BT_{c0}$ in terms of an underestimation of T_{c0} [18]. In the latter work, T_{c0} was associated with the onset of the resistance, rather than T_{BKT}. Here, we can exclude this possibility, as our analysis allows for an unambiguous determination of T_{BKT} and T_{c0}.

We theoretically describe the drop of $J_s(T)$, taking the BCS fit to $J_s(T)$ as input for the BKT renormalization group (RG) equations [8,45]. In this way, data is closely reproduced by RG theory (blue line in Fig. 3), assuming a vortex fugacity $\mu = 19$ K, or $\mu/J_s(0) \approx 2.5$, similar to values reported, e.g., in Ref. [10]. It is instructive to compare μ with the loss of condensation energy u_{cond} in the vortex cores with effective radius r_v. We write $u_{\mathrm{cond}} = \mu/(\pi r_v^2 d) \equiv B_c^2/2\mu_0 = [\hbar/(2\sqrt{2}e\xi\lambda)]^2/(2\mu_0)$, where B_c is the thermodynamic critical field. From the equation for μ, we find $r_v/\xi(T_{\mathrm{BKT}}) \simeq 2.2$. Using the expression $T_{\mathrm{BKT}} = T_{c0}(1 - 4Gi)$ with $Gi = 7e^2\zeta(3)R_N/(\pi^3h) = 0.0420$ being the Ginzburg-Levanyuk number [46], we expect $T_{\mathrm{BKT}}^{\mathrm{theo}} = 4.315$ K, which is only 4% smaller than $T_{\mathrm{BKT}} = 4.488$ K extracted from Fig. 3.

Finally, we investigate signatures of the BKT transition in magnetic field perpendicular to the film. In the high-field regime and near T_{BKT}, $R(B)$ is expected to cross over from sublinear to superlinear behavior [47], signaling a transition from amplitude fluctuations of the order parameter to vortex pinning. In Fig. 4(a) we observe such crossover at $T = 4.3$ K (blue line) slightly below the range extracted from the other observables. This discrepancy is probably caused by lack of thermal cycling between curves. For the low-field regime, Minnhagen has derived the scaling law [48]

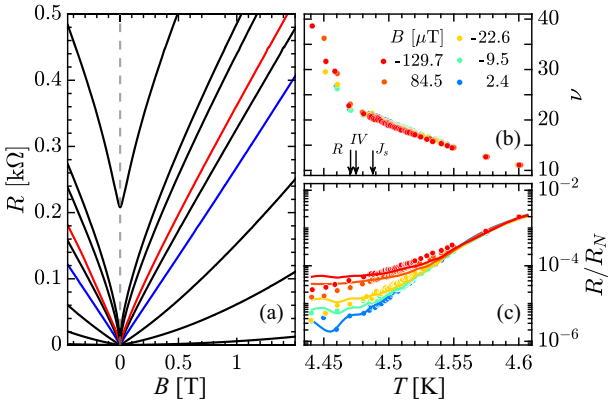

FIG. 4. (a) Magnetoresistance in the vicinity of T_{BKT} at different T. Curves correspond to temperatures (in K from top to bottom): 4.8, 4.6, 4.55, 4.4, 4.3, 4.0, 3.5, 2.5. Blue curve ($T = 4.3$ K) shows linear slope; red curve ($T = 4.45$ K) is closest to T_{BKT} from J_s. (b) Low-field magnetoresistance expressed in term of the scaling parameter $\nu(T)$ (see text). Arrows correspond to T_{BKT} from $R(T)$, $V(I)$, and $J_s(T)$, respectively. (c) $R(T)$ at very low fields together with the scaling function [Eq. (4)].

$$\frac{B}{B_{c2}} = \frac{R(B)}{R_N}\left[1 - \left(\frac{1}{\nu}\ln\frac{R(0)}{R_N}\right)^2\left(\frac{R(B)}{R_N}\right)^{-2/\nu}\right]^{1/2}, \quad (4)$$

where $B_{c2}(T) = \Phi_0/2\pi\xi^2(T)$ is the upper critical field and the scaling parameter ν is a universal function of T and B. In the Ginzburg-Landau limit, the coherence length can be written in the form $\xi(T) = \xi(T_{\mathrm{BKT}})[(T_{c0} - T_{\mathrm{BKT}})/(T_{c0} - T)]^{1/2}$. In Fig. 4(b) we show separately measured low-field data with field cooling procedure. From the measured $R(T, B)$ at fixed value of B, the function $\nu(T)$ can be determined from Eq. (4), if B_{c2} is given. Adjusting $B_{c2}(T_{\mathrm{BKT}}) = 6.1 \pm 1.7$ T leads to a collapse of the set of $\nu(T)$ curves at low field [Fig. 4(b)] that corresponds to a coherence length of $\xi(T_{\mathrm{BKT}}) = 6.7 \pm 0.6$ nm. The error margins mark a deviation from optimal scaling by one dot size. This implies that $\nu(T, B)$ only weakly depends on B. The BKT-transition temperature is reflected as a cusp in $\nu(T, B)$, which is located within 50 mK of T_{BKT} from the $R(T)$ curve [arrows in Fig. 4(b)].

We use the scaling function $\nu(T)$ in order to predict R vs T at very low B in Fig. 4(c). Our directly measured $R(T)$ (dots) and data obtained from the scaling expression of Eq. (4) (lines) agree well at the lowest B as slightly less at higher B.

Discussion.—The central result of our work is the observation of a sharp, textbook-like BKT transition in strongly disordered ultrathin NbN films. Hence, the previously observed broadening [10,13] is no genuine consequence of strong (but homogeneous) disorder in superconducting thin films. A possible explanation for the sharpness is a more homogenous distribution of defects in our ALD-deposited films, as opposed to the sputter deposited films in earlier works [17,18,44]. Long-range correlated disorder can explain the observed broadening of the transition in terms of a spatial variation of J_s [8,29,49]. On the other hand, short-range emergent granularity has been observed in STS for both sputter [17,50] and ALD [16] deposited films alike. At least at the level of disorder in our films, intrinsic inhomogeneity in the gap distribution appears to be irrelevant at the large length scales that determine the BKT transition. This finding aligns with previous Monte Carlo simulations conducted on two-dimensional effective XY models [29,51,52], which had highlighted that the mere presence of strong quenched disorder does not automatically lead to a broadening of the BKT transition. Instead, it is primarily the strong spatial correlation of the inhomogeneities that causes the smearing of the superfluid-stiffness jump at the critical point.

Most often, the presence of a BKT transition is deduced from the nonlinearity of $V(I)$ characteristics. However, this is not straightforward, as $V(I)$ often is strongly affected by heating phenomena. First, power-law behavior can also occur slightly above T_{BKT}, where only relatively few vortex-antivortex pairs are dissociated. A linear regime exists at the lowest currents only, while already at current densities $\lesssim 100$ A/m^2 current-induced dissociation dominates over thermal dissociation, leading to power-law behavior with $\alpha < 3$ that is not considered by standard theory.

These observations are important because a substantial fraction of the recent literature on ultrathin materials analyzes IV characteristics in the high-power regime above T_{BKT} in terms of BKT behavior (see, e.g., [53–59]). Our work shows that power-law exponents obtained in this regime are unrelated to BKT physics.

Conclusions.—We have shown that ultrathin superconducting films with strong, but homogeneous, disorder feature a sharp BKT transition without significant broadening. All relevant observables display quantitatively consistent results, allowing for a precise determination of the BKT- and mean-field transition temperatures as well as other parameters governing the films. Our study lays the ground for future controlled studies of the statics and dynamics of the BKT transition in ultrathin superconductors when approaching to the superconductor-insulator transition.

We would like to thank M. Ziegler and V. Ripka for NbN film deposition by ALD in the Leibniz IPHT clean room and E. König, I. Gornyi, A. Mirlin, P. Raychaudhuri, A. Ghosal, and F. Evers for helpful comments. The work was financially supported by the European Union's Horizon 2020 Research and Innovation Program under Grant Agreement No. 862660 QUANTUM E-LEAPS.

*These authors contributed equally to this work.
†christoph.strunk@ur.de

[1] J. M. Kosterlitz and D. J. Thouless, Ordering, metastability and phase transitions in two-dimensional systems, J. Phys. C **6**, 1181 (1973).

[2] J. M. Kosterlitz, The critical properties of the two-dimensional XY-model, J. Phys. C **7**, 1046 (1974).

[3] D. R. Nelson and J. M. Kosterlitz, Universal jump in the superfluid density of two-dimensional superfluids, Phys. Rev. Lett. **39**, 1201 (1977).

[4] D. McQueeney, G. Agnolet, and J. D. Reppy, Surface superfluidity in dilute ^{4}He-^{3}He mixtures, Phys. Rev. Lett. **52**, 1325 (1984).

[5] V. Ambegaokar, B. I. Halperin, D. R. Nelson, and E. D. Siggia, Dissipation in two-dimensional superfluids, Phys. Rev. Lett. **40**, 783 (1978).

[6] V. Ambegaokar, B. I. Halperin, D. R. Nelson, and E. D. Siggia, Dynamics of superfluid films, Phys. Rev. B **21**, 1806 (1980).

[7] B. I. Halperin and D. R. Nelson, Resistive transition in superconducting films, J. Low Temp. Phys. **36**, 599 (1979).

[8] L. Benfatto, C. Castellani, and T. Giamarchi, Broadening of the Berezinskii-Kosterlitz-Thouless superconducting transition by inhomogeneity and finite-size effects, Phys. Rev. B **80**, 214506 (2009).

[9] A. T. Fiory, A. F. Hebard, and W. I. Glaberson, Superconducting phase transitions in indium/indium-oxide thin-film composites, Phys. Rev. B **28**, 5075 (1983).

[10] J. Yong, T. R. Lemberger, L. Benfatto, K. Ilin, and M. Siegel, Robustness of the Berezinskii-Kosterlitz-Thouless transition in ultrathin NbN films near the superconductor-insulator transition, Phys. Rev. B **87**, 184505 (2013).

[11] G. Venditti, J. Biscaras, S. Hurand, N. Bergeal, J. Lesueur, A. Dogra, R. C. Budhani, M. Mondal, J. Jesudasan, P. Raychaudhuri, S. Caprara, and L. Benfatto, Nonlinear $I-V$ characteristics of two-dimensional superconductors: Berezinskii-Kosterlitz-Thouless physics versus inhomogeneity, Phys. Rev. B **100**, 064506 (2019).

[12] S. J. Turneaure, T. R. Lemberger, and J. M. Graybeal, Effect of thermal phase fluctuations on the superfluid density of two-dimensional superconducting films, Phys. Rev. Lett. **84**, 987 (2000).

[13] M. Mondal, S. Kumar, M. Chand, A. Kamlapure, G. Saraswat, G. Seibold, L. Benfatto, and P. Raychaudhuri, Role of the vortex-core energy on the Berezinskii-Kosterlitz-Thouless transition in thin films of NbN, Phys. Rev. Lett. **107**, 217003 (2011).

[14] A. Ghosal, M. Randeria, and N. Trivedi, Role of spatial amplitude fluctuations in highly disordered s-wave superconductors, Phys. Rev. Lett. **81**, 3940 (1998).

[15] A. Ghosal, M. Randeria, and N. Trivedi, Inhomogeneous pairing in highly disordered s-wave superconductors, Phys. Rev. B **65**, 014501 (2001).

[16] B. Sacépé, C. Chapelier, T. I. Baturina, V. M. Vinokur, M. R. Baklanov, and M. Sanquer, Disorder-induced inhomogeneities of the superconducting state close to the superconductor-insulator transition, Phys. Rev. Lett. **101**, 157006 (2008).

[17] C. Carbillet, S. Caprara, M. Grilli, C. Brun, T. Cren, F. Debontridder, B. Vignolle, W. Tabis, D. Demaille, L. Largeau, K. Ilin, M. Siegel, D. Roditchev, and B. Leridon, Confinement of superconducting fluctuations due to emergent electronic inhomogeneities, Phys. Rev. B **93**, 144509 (2016).

[18] C. Carbillet, V. Cherkez, M. A. Skvortsov, M. V. Feigel'man, F. Debontridder, L. B. Ioffe, V. S. Stolyarov, K. Ilin, M. Siegel, D. Roditchev, T. Cren, and C. Brun, Spectroscopic evidence for strong correlations between local superconducting gap and local Altshuler-Aronov density of states suppression in ultrathin NbN films, Phys. Rev. B **102**, 024504 (2020).

[19] M. Stosiek, B. Lang, and F. Evers, Self-consistent-field ensembles of disordered Hamiltonians: Efficient solver and application to superconducting films, Phys. Rev. B **101**, 144503 (2020).

[20] R. W. Crane, N. P. Armitage, A. Johansson, G. Sambandamurthy, D. Shahar, and G. Grüner, Fluctuations, dissipation, and nonuniversal superfluid jumps in two-dimensional superconductors, Phys. Rev. B **75**, 094506(R) (2007).

[21] S. Mandal, S. Dutta, S. Basistha, I. Roy, J. Jesudasan, V. Bagwe, L. Benfatto, A. Thamizhavel, and P. Raychaudhuri, Destruction of superconductivity through phase fluctuations in ultrathin a-MoGe films, Phys. Rev. B **102**, 060501(R) (2020).

[22] D. M. Broun, W. A. Huttema, P. J. Turner, S. Özcan, B. Morgan, R. Liang, W. N. Hardy, and D. A. Bonn, Superfluid density in a highly underdoped $YBa_2Cu_3O_{6+y}$ superconductor, Phys. Rev. Lett. **99**, 237003 (2007).

[23] S. Kamal, D. A. Bonn, N. Goldenfeld, P. J. Hirschfeld, R. Liang, and W. N. Hardy, Penetration depth measurements of 3D XY critical behavior in $YBa_2Cu_3O_{6.95}$ crystals, Phys. Rev. Lett. **73**, 1845 (1994).

[24] J. Yong, M. J. Hinton, A. McCray, M. Randeria, M. Naamneh, A. Kanigel, and T. R. Lemberger, Evidence of two-dimensional quantum critical behavior in the superfluid density of extremely underdoped $Bi_2Sr_2CaCu_2O_{8+x}$, Phys. Rev. B **85**, 180507(R) (2012).

[25] Y. Zuev, M. S. Kim, and T. R. Lemberger, Correlation between superfluid density and T_c of underdoped $YBa_2Cu_3O_{6+x}$ near the superconductor-insulator transition, Phys. Rev. Lett. **95**, 137002 (2005).

[26] K. Medvedyeva, B. J. Kim, and P. Minnhagen, Analysis of current-voltage characteristics of two-dimensional superconductors: Finite-size scaling behavior in the vicinity of the Kosterlitz-Thouless transition, Phys. Rev. B **62**, 14531 (2000).

[27] R. Ganguly, D. Chaudhuri, P. Raychaudhuri, and L. Benfatto, Slowing down of vortex motion at the Berezinskii-Kosterlitz-Thouless transition in ultrathin NbN films, Phys. Rev. B **91**, 054514 (2015).

[28] S. Mallik, G. Ménard, G. Saïz, H. Witt, J. Lesueur, A. Gloter, L. Benfatto, M. Bibes, and N. Bergeal, Superfluid stiffness of a $KTaO_3$-based two-dimensional electron gas, Nat. Commun. **13**, 4625 (2022).

[29] I. Maccari, L. Benfatto, and C. Castellani, Broadening of the Berezinskii-Kosterlitz-Thouless transition by correlated disorder, Phys. Rev. B **96**, 060508(R) (2017).

[30] I. Tamir, A. Benyamini, E. J. Telford, F. Gorniaczyk, A. Doron, T. Levinson, D. Wang, F. Gay, B. Sacepe, J. Hone, K. Watanabe, T. Taniguchi, C. R. Dean, A. N. Pasupathy, and D. Shahar, Sensitivity of the superconducting state in thin films, Sci. Adv. **5**, eaau3826 (2019).

[31] A. Benyamini, E. J. Telford, D. M. Kennes, D. Wang, A. Williams, K. Watanabe, T. Taniguchi, D. Shahar, J. Hone, C. R. Dean, A. J. Millis, and A. N. Pasupathy, Fragility of

the dissipationless state in clean two-dimensional superconductors, Nat. Phys. **15**, 947 (2019).
[32] T. Levinson, A. Doron, F. Gorniaczyk, and D. Shahar, Electron-phonon coupling across the superconductor-insulator transition, Phys. Rev. B **100**, 184508 (2019).
[33] S. Linzen, M. Ziegler, O. V. Astafiev, M. Schmelz, U. Hübner, M. Diegel, E. Il'ichev, and H.-G. Meyer, Structural and electrical properties of ultrathin niobium nitride films grown by atomic layer deposition, Supercond. Sci. Technol. **30**, 035010 (2017).
[34] C. Baumgartner, L. Fuchs, L. Frész, S. Reinhardt, S. Gronin, G. C. Gardner, M. J. Manfra, N. Paradiso, and C. Strunk, Josephson inductance as a probe for highly ballistic semiconductor-superconductor weak links, Phys. Rev. Lett. **126**, 037001 (2021).
[35] See Supplemental Material at http://link.aps.org/supplemental/10.1103/PhysRevLett.131.186002 for further details, which includes Refs. [36,37].
[36] J. M. B. Lopes dos Santos and E. Abrahams, Superconducting fluctuation conductivity in a magnetic field in two dimensions, Phys. Rev. B **31**, 172 (1985).
[37] M. Tinkham, *Introduction to Superconductivity* (McGraw-Hill, New York, 1996).
[38] M. Mondal, A. Kamlapure, M. Chand, G. Saraswat, S. Kumar, J. Jesudasan, L. Benfatto, V. Tripathi, and P. Raychaudhuri, Phase fluctuations in a strongly disordered *s*-wave NbN superconductor close to the metal-insulator transition, Phys. Rev. Lett. **106**, 047001 (2011).
[39] T. I. Baturina, S. V. Postolova, A. Y. Mironov, A. Glatz, M. R. Baklanov, and V. M. Vinokur, Superconducting phase transitions in ultrathin TiN films, Europhys. Lett. **97**, 17012 (2012).
[40] S. V. Postolova, A. Y. Mironov, and T. I. Baturina, Non-equilibrium transport near the superconducting transition in TiN films, JETP Lett. **100**, 635 (2015).
[41] A. Yu. Mironov, S. V. Postolova, and T. I. Baturina, Quantum contributions to the magnetoconductivity of critically disordered superconducting TiN films, J. Phys. Condens. Matter **30**, 485601 (2018).
[42] K. Kronfeldner, T. I. Baturina, and C. Strunk, Multiple crossing points and possible quantum criticality in the magnetoresistance of thin TiN films, Phys. Rev. B **103**, 184512 (2021).
[43] A. I. Larkin and A. Varlamov, *Theory of Fluctuations in Superconductors* (Clarendon Press, Oxford, 2005).
[44] A. Semenov, B. Günther, U. Böttger, H.-W. Hübers, H. Bartolf, A. Engel, A. Schilling, K. Ilin, M. Siegel, R. Schneider, D. Gerthsen, and N. A. Gippius, Optical and transport properties of ultrathin NbN films and nanostructures, Phys. Rev. B **80**, 054510 (2009).
[45] I. Maccari, N. Defenu, L. Benfatto, C. Castellani, and T. Enss, Interplay of spin waves and vortices in the two-dimensional XY model at small vortex-core energy, Phys. Rev. B **102**, 104505 (2020).
[46] E. J. König, A. Levchenko, I. V. Protopopov, I. V. Gornyi, I. S. Burmistrov, and A. D. Mirlin, Berezinskii-Kosterlitz-Thouless transition in homogeneously disordered superconducting films, Phys. Rev. B **92**, 214503 (2015).
[47] J. C. Garland and H. J. Lee, Influence of a magnetic field on the two-dimensional phase transition in thin-film superconductors, Phys. Rev. B **36**, 3638 (1987).
[48] P. Minnhagen, Evidence of magnetic field scaling for two-dimensional superconductors, Phys. Rev. B **29**, 1440 (1984).
[49] L. Benfatto, C. Castellani, and T. Giamarchi, Berezinskii–Kosterlitz–Thouless transition within the sine-Gordon approach: The role of the vortex-core energy, 40 Years of Berezinskii–Kosterlitz–Thouless Theory (World Scientific Publishing Co, Singapore, 2013), pp. 161–199.
[50] A. Kamlapure, T. Das, S. C. Ganguli, J. B. Parmar, S. Bhattacharyya, and P. Raychaudhuri, Emergence of nanoscale inhomogeneity in the superconducting state of a homogeneously disordered conventional superconductor, Sci. Rep. **3**, 2979 (2013).
[51] I. Maccari, L. Benfatto, and C. Castellani, The BKT universality class in the presence of correlated disorder, Condens. Matt. **3**, 8 (2018).
[52] I. Maccari, L. Benfatto, and C. Castellani, Disordered XY model: Effective medium theory and beyond, Phys. Rev. B **99**, 104509 (2019).
[53] N. Reyren, S. Thiel, A. D. Caviglia, L. F. Kourkoutis, G. Hammerl, C. Richter, C. W. Schneider, T. Kopp, A.-S. Rüetschi, D. Jaccard, M. Gabay, D. A. Muller, J.-M. Triscone, and J. Mannhart, Superconducting interfaces between insulating oxides, Science **317**, 1196 (2007).
[54] Z. Wen-Hao *et al.*, Direct observation of high-temperature superconductivity in one-unit-cell FeSe films, Chin. Phys. Lett. **31**, 017401 (2014).
[55] J. M. Lu, O. Zheliuk, I. Leermakers, N. F. Q. Yuan, U. Zeitler, K. T. Law, and J. T. Ye, Evidence for two-dimensional Ising superconductivity in gated MoS_2, Science **350**, 1353 (2015).
[56] Y. Cao, V. Fatemi, S. Fang, K. Watanabe, T. Taniguchi, E. Kaxiras, and P. Jarillo-Herrero, Unconventional superconductivity in magic-angle graphene superlattices, Nature (London) **556**, 43 (2018).
[57] J. M. Park, Y. Cao, K. Watanabe, T. Taniguchi, and P. Jarillo-Herrero, Tunable strongly coupled superconductivity in magic-angle twisted trilayer graphene, Nature (London) **590**, 249 (2021).
[58] H. Zhou, T. Xie, T. Taniguchi, K. Watanabe, and A. F. Young, Superconductivity in rhombohedral trilayer graphene, Nature (London) **598**, 434 (2021).
[59] E. Zhang *et al.*, Spin–orbit–parity coupled superconductivity in atomically thin 2M-WS_2, Nat. Phys. **19**, 106 (2023).